Differential Distribution of Subsets of Myofibrillar Proteins In Cardiac Nonstriated and Striated Myofibrils

Thomas Schultheiss,* Zhongxiang Lin,*‡ Mei-Hua Lu,* John Murray,* Donald A. Fischman,§ Klaus Weber,‖ Tomoh Masaki,¶ Michihiro Imamura,¶ and Howard Holtzer*

*Department of Anatomy, School of Medicine, University of Pennsylvania, Philadelphia, Pennsylvania 19104; ‡Department of Cell Biology, Beijing Institute for Cancer Research, Beijing, China; §Department of Cell Biology and Anatomy, Cornell University Medical College, New York 10021; ‖Max Planck Institute for Biophysical Chemistry, Goettingen, Federal Republic of Germany; and ¶ Institute of Basic Medical Sciences, University of Tsukaba, Tsukaba, Japan

Abstract. Cultured cardiac myocytes were stained with antibodies to sarcomeric α-actinin, troponin-I, α-actin, myosin heavy chain (MHC), titin, myomesin, C-protein, and vinculin. Attention was focused on the distribution of these proteins with respect to nonstriated myofibrils (NSMFs) and striated myofibrils (SMFs). In NSMFs, α-actinin is found as longitudinally aligned, irregular ~0.3-μm aggregates. Such aggregates are associated with α-actin, troponin-I, and titin. These I-Z-I–like complexes are also found as ectopic patches outside the domain of myofibrils in close apposition to the ventral surface of the cell. MHC is found outside of SMFs in the form of discrete fibrils. The temporal–spatial distribution and accumulation of the MHC-fibrils with respect to the I-Z-I–like complexes varies greatly along the length of the NSMFs. There are numerous instances of I-Z-I–like complexes without associated MHC-fibrils, and also cases of MHC-fibrils located many microns from I-Z-I–like complexes. The transition between the terminal ~1.7-μm sarcomere of any given SMF and its distal NSMF-tip is abrupt and is marked by a characteristic narrow α-actinin Z-band and vinculin positive adhesion plaque.

A titin antibody T20, which localizes to an epitope at the Z-band in SMFs, precisely costains the 0.3-μm α-actinin aggregates in ectopic patches and NSMFs. Another titin antibody T1, which in SMFs localizes to an epitope at the A-I junction, typically does not stain ectopic patches and NSMFs. Where detectable, the T1-positive material is adjacent to rather than part of the 0.3-μm α-actinin aggregates. Myomesin and C-protein are found only in their characteristic sarcomeric locations (even in just perceptible SMFs). These A-band–associated proteins appear to be absent in ectopic patches and NSMFs.

From the point of view of both development (8, 19, 20, 22) and evolution (14), striated myofibrils are strikingly conservative structures. Within the past decade, the sequences of over two dozen myofibrillar genes have been described. Several of these genes are remarkably responsive to intracellular transacting factors (7, 41) including oncogenes (1, 21), as well as to a variety of extracellular molecules such as hormones (39), neural transmitters (37), phorbol esters (29, 30), and carcinogens (3). During this period, less attention has been directed to the time, place, and conditions that permit the newly synthesized proteins encoded by these genes to assemble into invariant tandem sarcomeres.

Earlier studies have demonstrated the following: postmitotic, mononucleated skeletal myoblasts and cardiac myocytes, in vivo and in vitro, synthesize sarcomeric myosin heavy and light chains, α-actin, sarcomeric α-actinin, myomesin, C-protein, and titin, as well as desmin (6, 10–12, 16, 18–24). The earliest longitudinal alignment of myofibrillar proteins occurs in proximity to subsarcolemmal stress fiber-like structures and is first observed in 10–15-h-old postmitotic, mononucleated myoblasts (3, 11, 19, 20, 34). These transitory nonstriated myofibrils (NSMFs)[1] consist of a tangle of overlapping arrays of ~1.6-μm-long-thick filaments and I-Z-I-like complexes, along with cytoskeletal thin filaments and dense bodies consisting of β- and γ-actins, cytoskeletal myosin heavy chain (MHC), and cytoskeletal α-actinin (11, 23, 27, 36). Within the next 15–30 h, the cytoskeletal structures disappear and the loosely aligned myofibrillar structures that constitute the NSMFs appear to sort out into nascent striated myofibrils (SMFs) made up of typical ~1.7-μm sarcomeres. Sarcomeres <~1.7 μm in length are never observed (3, 11, 18–21, 30). Newly assembled sarcomeres consist of laterally aligned 1.6-μm-long thick filaments that interdigitate with polarized 1.0-μm-long thin filaments. Most often the proximal part of a given nascent myofibril is striated, whereas distally both ends are often nonstriated and

1. *Abbreviations used in this paper*: MHC, myosin heavy chain; NSMF, nonstriated myofibrils; SMF, striated myofibrils.

terminate in adhesion plaques and/or intercalated disks, complexes of vinculin/sarcomeric α-actinin/α-actin (9, 30, 42).

We have been examining the temporal and spatial distribution of several myofibrillar proteins during the early stages of myofibrillogenesis in cultured cardiac myocytes (8, 11, 30). Between culture days 3 and 7, the myocytes flatten, increase their sarcomeric MHC and α-actin 8–10-fold and increase the number, length and diameter of their nascent myofibrils. By double staining myocytes with labeled antibodies, we have made the following observations: (*a*) the spatial deployment of sarcomeric MHC, myomesin, C-protein, α-actin, sarcomeric α-actinin, troponin-I, and titin in the earliest assembled ~1.7-μm sarcomeres in nascent SMFs is indistinguishable from their respective deployment in sarcomeres in adult SMFs; (*b*) in contrast, NSMFs consist of linearly disposed, irregular ~0.3-μm α-actinin aggregates that costain with antibodies to α-actin, troponin-I, and titin; (*c*) these I-Z-I–like complexes loosely associate with varying numbers of MHC-containing fibrils; (*d*) regions outside the domains of either SMFs or NSMFs assemble ectopic I-Z-I–like complexes that lack MHC-fibrils; (*e*) antibodies to different titin epitopes stain I-Z-I–like complexes differently. One antibody T20 costains α-actinin Z-bands and 0.3-μm aggregates. The other T1 stains delicate doublets around Z-bands and is usually undetectable in NSMFs or, when present, does not colocalize with the α-actinin aggregates; (*f*) NSMFs differ from SMFs in that they do not bind antibodies to myomesin or C-protein, the epitopes for these proteins being detected only within fully assembled ~1.7-μm sarcomeres where they exhibit their characteristic positions; (*g*) the transition between NSMFs and SMFs is abrupt, with the SMF ending in a sharp Z-band; and (*h*) both NSMFs and SMFs associate with vinculin positive plaques, but these structures are particularly prominent at the NSMF/SMF transition zone.

Materials and Methods

Cell Culture

Chick cardiac cultures were prepared from 5–7 d embryos and grown on glass coverslips as previously described (30). All observations were made on day 5–7 cultures.

Antibodies

Monoclonal antisarcomeric MHC (F4G3), a generous gift from Dr. F. Pepe of the University of Pennsylvania, and polyclonal antilight meromyosin recognize MHC from cardiac and skeletal muscle cells only (2, 29, 30). Two antibodies to muscle-specific α-actinin were used: a monoclonal antibody (9A2B8) and an affinity-purified polyclonal antibody (12). Both recognize α-actinin from cardiac and skeletal muscle, but do not recognize any proteins from smooth muscle or nonmuscle cells (12, 30). A rabbit polyclonal antiskeletal troponin is a gift from Dr. S. Hitchcock-DeGregori, University of Medicine and Dentistry, New Jersey. In immunoblots at the concentration used (1:3,000), this antibody binds to troponin-I but not troponin-T or -C or actin. This antibody stains I-bands in all skeletal myotubes and in roughly 20% of the cultured cardiac myocytes. Monoclonal anti-α-actin (B4) is a gift from Dr. J. Lessard, University of Cincinnati, Ohio. It recognizes all α-actin isoforms and also γ smooth muscle actin (28). Monoclonal anti-titin T1 and T20 recognize epitopes at the A-I junction and Z-line, respectively, in striated skeletal and cardiac muscle cells (13). Three different monoclonal antibodies to myomesin were used: Cp-13 (14), and B4 and B5 (16), the latter two being generous gifts from Dr. H. Eppenberger (ETH, Zurich, Switzerland). Monoclonal anti-C-protein (MF-1) stains the A-bands of striated myofibrils (33). The mAb against chicken gizzard vinculin was purchased from ICN Immunochemicals (Lisle, IL) (Clone No. 11-5).

Immunofluorescence Staining and Microscopy

Cells were fixed and processed for double-staining as described in detail by Lin et al. (29, 30). Affinity-purified rhodamine and fluorescein-tagged secondary antibodies were purchased from Cooper Biochemical (Malvern, PA) except for rhodamine goat anti-rabbit, which was purchased from Kirkegaard and Perry (Gaithersberg, MD). Some cells were stained with rhodamine-labeled phalloidin (Molecular Probes Inc., Eugene, OR) at a concentration of 1:100 in PBS at room temperature for 20 min. Cells were mounted in 60% glycerol and 2.5% 1,4-diazabicyclo (2.2.2) octane (DABCO; Sigma Chemical Co., St. Louis, MO) in PBS to prevent bleaching.

Most cells were examined with a Zeiss epifluorescence microscope, using a combination of rhodamine and fluorescein excitation and barrier filter sets that eliminate virtually all bleed-through between channels. Photographs were taken with Kodak T-Max 400 ASA film.

For video microscopy, cells were illuminated using an Olympus inverted microscope equipped with epifluorescence and the same Zeiss filters as above. Images were collected using a SIT-camera (model 65; Dage-MTI, Inc., Wabash, MI) in manual mode, averaging over 256 frames, and Gould image processing software. Images were also collected without illumination for the purpose of background subtraction, and images of uniform fields of rhodamine and fluorescein dye were collected for the purpose of detecting nonuniformities in illumination or camera sensitivity across the microscopic field. Images were corrected for background and uneven field illumination or sensitivity on a pixel-by-pixel basis by subtracting the background and dividing by the image of the appropriate uniform field of dye. Intensities of individual pixels in the corrected images were determined using Gould image processing software. The size of the pixels was small compared to the smallest objects measured (at least 10 pixels in the ~0.3 μm α-actinin aggregates).

It is difficult to make reliable and reproducible measurements under the fluorescence microscope. Z-bands that in EM sections measure 0.1 μm in width measure over 0.2 μm in the fluorescence microscope after staining with anti-α-actinin. Nascent A-bands that in EM sections consist of aligned 1.6-μm-long thick filaments appear longer after staining with anti-MHC. To avoid confusion in the following, the size of fluorescent A-bands is taken as 1.6-μm-long, and the size of all other fluorescent objects estimated accordingly.

Figure 1. (*a* and *b*) Cultured day 5 myocytes double-stained to illustrate not only SMFs and NSMFs, but also the considerable variability in the degree of branching of myofibrils in different cardiac myocytes. Arrows in *a* and *b*, point to the NSMFs at the distal ends, and to the transitory intercalated, nonstriated stretches along the length of SMFs. Both NSMFs and intercalated nonstriated stretches stain discontinuously with anti-α-actinin (*a*, *fluorescein channel*), whereas these same regions stain continuously with rho-phalloidin (*b*). Note that in many of the rho-phalloidin–stained I-Z-I complexes the Z-band is slightly more fluorescent that the inserted thin filaments. Asterisks in *a* and *b*, mark a fibroblast with out-of-focus stress fibers. (*c* and *d*) A myocyte double-stained with anti-α-actinin (Fig. 1 *c*; *fluorescein channel*) and rho-phalloidin (*d*). At the right margin a group of SMFs is shown with typical narrow α-actinin Z-bands (*C*). Within this same group of SMFs, rho-phalloidin stains the thin filaments in each successive I-Z-I complex (*d*). The nonfluorescent stripe between each stained I-Z-I complex in *d* marks the H-zone of each A-band. A cluster of NSMFs and ectopic patches indicated by the two sets of left arrows stain discontinuously with anti-α-actinin but continuously with rho-phalloidin. The blurred fluorescence at the top and at the left margin in *d* (*asterisks*) is because of out-of-focus stress fibers in neighboring fibroblasts. Note that the sarcomeric anti-α-actinin

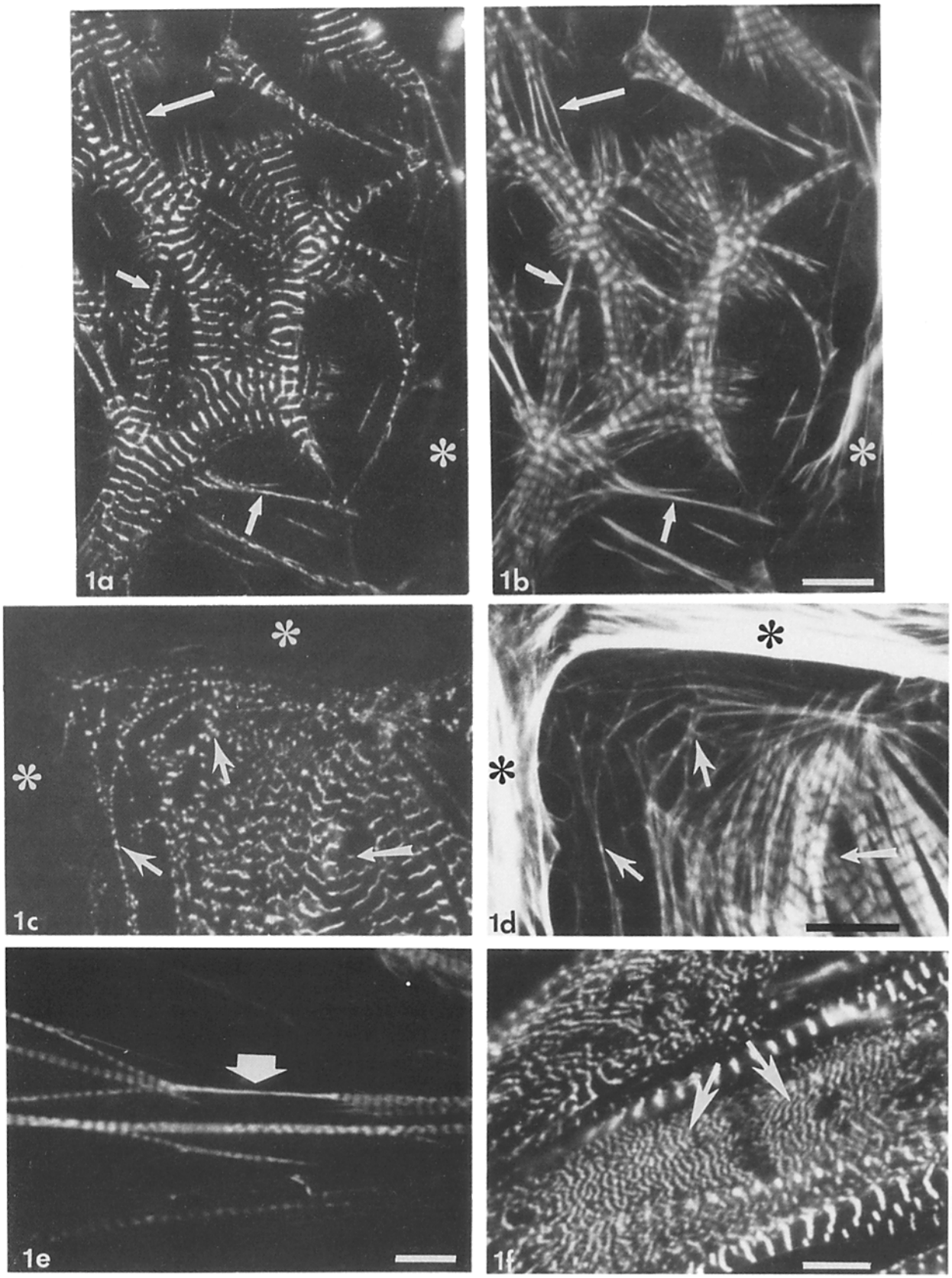

does not stain the cytoskeletal α-actinin dense bodies in the stress fibers of these fibroblasts. (*e*) A cardiac myocyte stained with anti-α-actin. The antibody stains the I-Z-I complexes of SMFs, whereas it stains both NSMFs and nonstriated interspersed stretches intensely and in a uniform, linear pattern (*arrow*). (*f*) A cardiac myocyte stained with anti-α-actinin to illustrate the ectopic patch arrangement of α-actinin aggregates (*arrows*). The ectopic patches are always located in close apposition to the ventral plasma membrane. Such ectopic patches are often devoid of MHC fibrils. Bars, 10 μm.

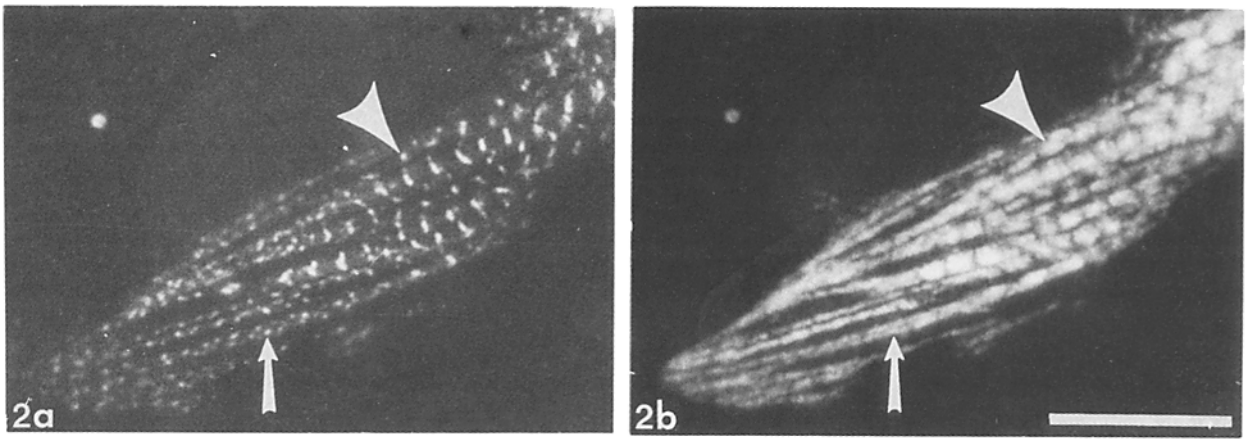

Figure 2. A myocyte double-stained with anti-α-actinin (*a, fluorescein channel*) and anti-troponin-I (*b, rhodamine channel*). Anti-troponin-I stains thin filaments in each I-Z-I complex in a pattern similar to that revealed with rho-phalloidin. The distal NSMFs that stain discontinuously with anti-α-actinin stain more continuously with anti-troponin-I. Bar, 10 μm.

Results

Distribution of I-Z-I Proteins MHC and Vinculin with respect to NSMFs and SMFs

To visualize the distribution of myofibrillar proteins of the I-Z-I complex in NSMFs and SMFs, day 3–7 cultures were stained with antibodies to sarcomeric α-actinin, troponin-I, and α-actin, as well as with rho-phalloidin.

Fig. 1 (*A–D*) illustrates a large part of the range of structures that stain with anti-α-actinin and rho-phalloidin. Both proximal nascent SMFs and their distal NSMFs can be observed. The respective patterns of the anti-α-actinin-stained Z-bands and the rho-phalloidin–stained I-Z-I complexes in the newly assembled SMFs are identical to those in adult sarcomeres. NSMFs stained with anti-α-actinin display a punctuate or discontinuous pattern consisting of numerous, closely spaced irregular ± 0.3-μm aggregates, whereas when costained with rho-phalloidin they appear as continuously fluorescent structures (see also below). (As the apparent size is affected by the intensity of the fluorescent signal, it is likely that the actual size of these irregular α-actinin aggregates is <0.3 μm. See Materials and Methods.) In addition, α-actinin aggregates are often observed as ectopic patches beyond the boundaries of either SMFs or NSMFs (Fig. 1 *F*). Such ectopic patches are closely applied to the ventral surface of the cell. Arrangements of α-actinin that fall in between the categories of NSMF and ectopic patch are also common. In general, NSMFs are more linear and are continuous with SMFs, whereas ectopic patches are less linear and are located more peripherally in the cell. Not infrequently during early stages of myofibrillogenesis a given SMF, consisting of typically spaced A-, I-, and Z-bands, exhibits interspersed nonstriated stretches (Fig. 1, *A*, *B*, and *E*). Such interspersed nonstriated stretches are similar in staining properties to the distal NSMFs. Both the distal NSMFs and the nonstriated interspersed stretches disappear as the myofibrils mature. We interpret these changes as indicating that the proteins in both regions undergo rearrangement and translocate, eventually assembling into typical ~1.7-μm sarcomeres (3, 11, 19, 20, 22, 34).

In the current study, we have used an affinity-purified antibody that recognizes α-actinin only from skeletal and cardiac muscle cells, and not from smooth muscle or nonmuscle cells (12, 30). The current results indicate that the sarcomeric isoform of α-actinin is present in a range of nonstriated structures located extensively throughout the myocyte. An antibody that recognizes α-actinin from both muscle and nonmuscle cells (30) stains cardiac cells in an identical manner to the sarcomeric α-actinin antibody used in Fig. 1 (data not shown), suggesting that the sarcomeric isoform of α-actinin is present in all α-actinin containing structures in cardiac muscle cells. Note that the distribution of the aggregates of sarcomeric α-actinin is similar to that observed following the microinjection of nonsarcomeric or sarcomeric α-actinin into living myogenic cells (32, 40).

Figure 3. (*a–h*) Double-stained myocytes from day 5 cultures. *a*, *c*, *e*, and *g* are stained with anti-α-actinin (*rhodamine channel*), *b*, *d*, *f*, and *h* with anti-MHC (*fluorescein channel*). *a* and *b* illustrate the abrupt transition between SMFs and NSMFs in the growth tip of a myocyte. Although the density of the ± 0.3-μm α-actinin aggregates and the MHC fibrils varies along the length of the NSMFs, both proteins are present throughout and are roughly coterminous. The large, fluorescent circle in *a* is an artifact. *c* and *d* illustrate that longitudinally oriented clusters of MHC-fibrils can assemble at distances of up to 5–6-μm from α-actinin–positive SMFs and NSMFs. Arrows point to intercalated, nonstriated stretches. *e* and *f* illustrate an ectopic patch positive for both ± 0.3-μm α-actinin aggregates and MHC fibrils. In this instance the ~1.6-μm-long MHC fibrils appear to be randomly oriented. We do not know the minimal number of 1.6-μm-long thick filaments required to be recognizable as a cluster of MHC fibrils. *g* and *h* illustrate the more common relationships between groups of MHC fibrils and α-actinin ectopic patches. The ectopic patch is positive for ± 0.3-μm α-actinin aggregates but totally negative for MHC fibrils. Left arrow points to 4 successive Z-bands and their accompanying MHC fibrils packed into definitive A-bands. Right arrow points, not to ~1.7-μm spaced Z-bands, but to linearly distributed ± 0.3-μm aggregates. Note no MHC fibrils associate with this latter structure. Bars, 10 μm.

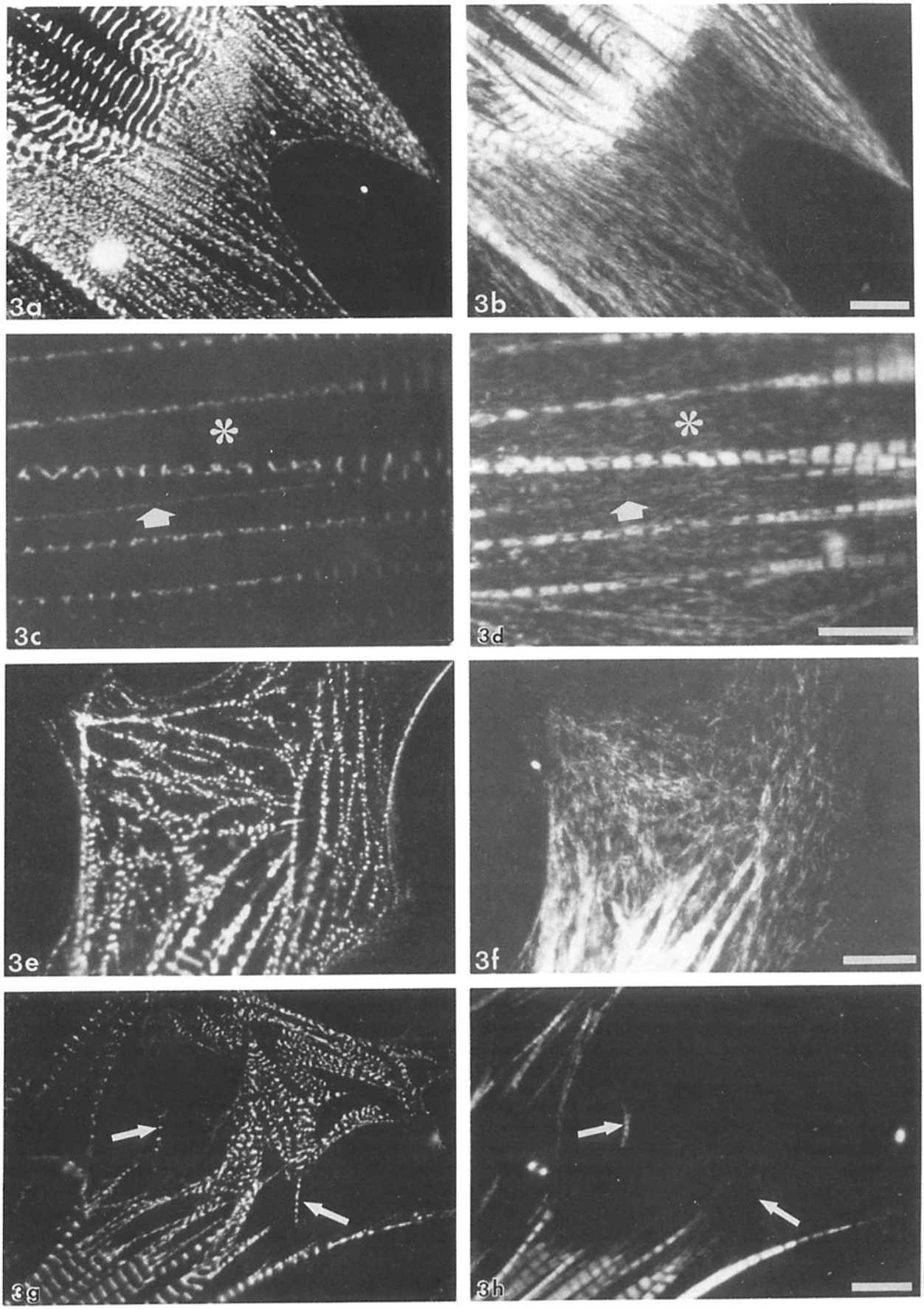
3a
3b
3c
3d
3e
3f
3g
3h

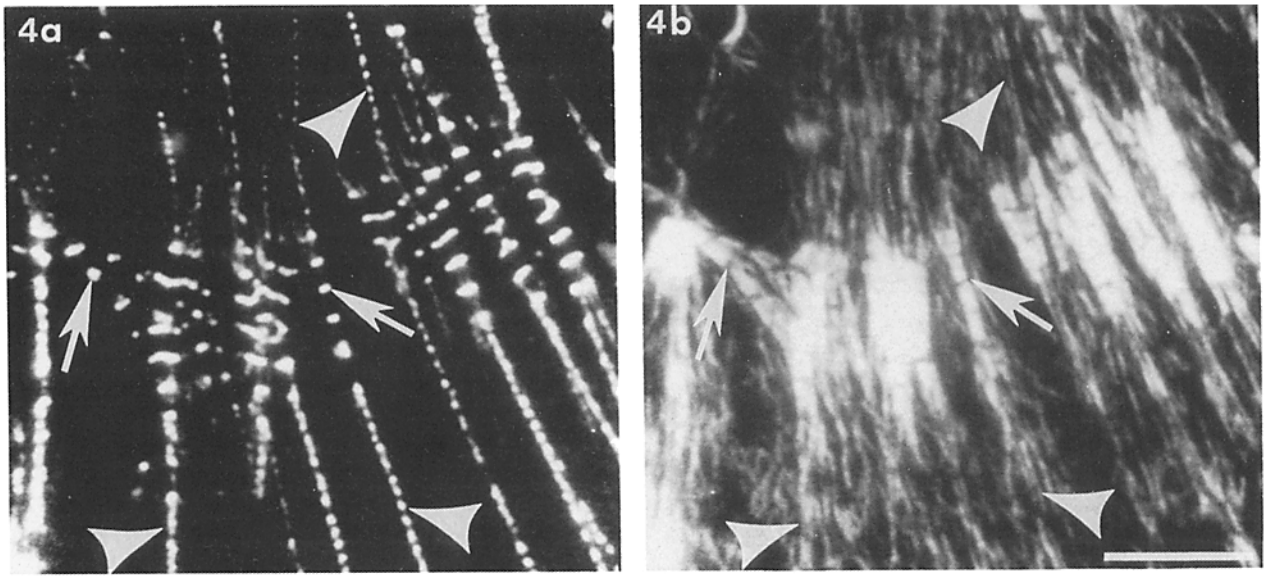

Figure 4. (*a* and *b*) High magnification images of a myocyte double-stained with sarcomeric anti-α-actinin (*a, rhodamine channel*) and anti-MHC (*b, fluorescein channel*). Images were recorded with a video camera averaging over 256 frames, followed by background subtraction and gain normalization to correct for uneven illumination and camera sensitivity. Arrows point to ~1.7-μm-long sarcomeres, whereas arrowheads indicate NSMFs. Note that the α-actinin in the NSMFs is confined to discrete arrays of ± 0.3-μm aggregates while the MHC-positive material consists of a much looser arrangement of MHC fibrils. Regions lacking α-actinin aggregates are often filled with MHC fibrils. To define better the scattered clusters of MHC fibrils, the intensely fluorescent 1.6-μm A-bands were overexposed. Average fluorescence intensities over a box of 3 × 4 pixels were measured for several of the sarcomeric Z-bands and the nonsarcomeric α-actinin aggregates in Fig. 3 *a*. The objects measured were always larger than the boxes. The intensity ranges of the Z-bands and the α-actinin aggregates were found to overlap greatly, with some Z-bands more intense and others less intense than many of the aggregates (data not shown). Bars, 10 μm.

Double staining with anti-α-actinin and phalloidin indicates that the sarcomeric α-actinin of nonstriated structures is always associated with actin (Fig. 1, *A–D*). Staining with anti-α-actin indicates that distal NSMFs or interspersed nonstriated stretches that would stain discontinuously with anti-α-actinin stain continuously for α-actin (Fig. 1 *E*). Furthermore, the α-actinin aggregates of nonstriated structures are always associated with troponin-I (Fig. 2). The troponin-I antibody also stains the NSMFs and ectopic patches more continuously than the anti-α-actinin. In brief, whether in SMFs, NSMFs, or in ectopic patches, sarcomeric α-actinin is always found complexed with α-actin and troponin-I. These findings suggest that at least partially assembled thin filaments (e.g., α-actin polymers plus troponin-I) complex with α-actinin aggregates to form I-Z-I–like complexes and that these constitute the bulk of both NSMFs and ectopic patches. The I-Z-I–like complexes also contain titin (see below).

We next determined the relationship between the I-Z-I–like complexes and myosin. Previous work has indicated that sarcomeric myosin may be associated with NSMFs (3, 11, 40), but the extent of this relationship is not known. Figs. 3, (*A–H*) and 4 illustrate the variations in distribution of α-actinin and MHC in SMFs and NSMFs. Note that anti-MHC does not stain NSMFs diffusely; rather, anti-MHC binds to fine fibrils. In fluorescence micrographs, because of such variables as orientation and overlap of structures, it is difficult to determine precisely the length of the MHC fibrils, but many appear to approach the length of thick filaments in A-bands. Electron microscopy studies are currently underway to determine more precisely the lengths of the MHC fibrils. MHC fibrils and α-actinin aggregates are often abundant near the transition zones between SMFs and NSMFs (Fig. 3, *A* and *B*). However, the localization of MHC with respect to α-actinin can vary greatly, both between different individual NSMFs as well as along the length of a given NSMF (Figs. 3, *A–D*, and 4, *A–B*). In some areas of the cell MHC fibrils, many microns from all α-actinin aggregates can be found (Fig. 3, *C* and *D*), and stretches of over 30 μm along a given NSMF can be totally free of MHC fibrils. Most frequently MHC fibrils are absent from ectopic patches (Figs. 3, *G* and *H*), although instances of patches exhibiting MHC fibrils occur (Figs. 3, *E* and *F*).

Previous studies suggest that NSMFs and ectopic patches that do not stain with sarcomeric MHC antibodies would stain with antibodies to nonmuscle myosin (11). Since monoclonal antibodies specific to subsets of sarcomeric MHC molecules have been reported (47), it is also possible that these nonstriated structures contain a sarcomeric myosin that is not recognized by our MHC antibody. The latter possibility seems unlikely, however, since our MHC antibody stains all cultured cardiac and skeletal muscle cells, including myotomal, postmitotic myoblasts (8, 19, 20), and stage 10 embryonic chick cardiac cells (T. S. Schultheiss, H. Holtzer, unpublished observations).

The in vivo and in vitro relationships among intercalated discs, NSMFs and SMFs have yet to be unravelled (4, 30, 36, 42). Fig. 5, *A–D*, illustrate that the most distal sarcomeres of any given SMF insert into a vinculin positive plaque similar in morphology to those found at the termini

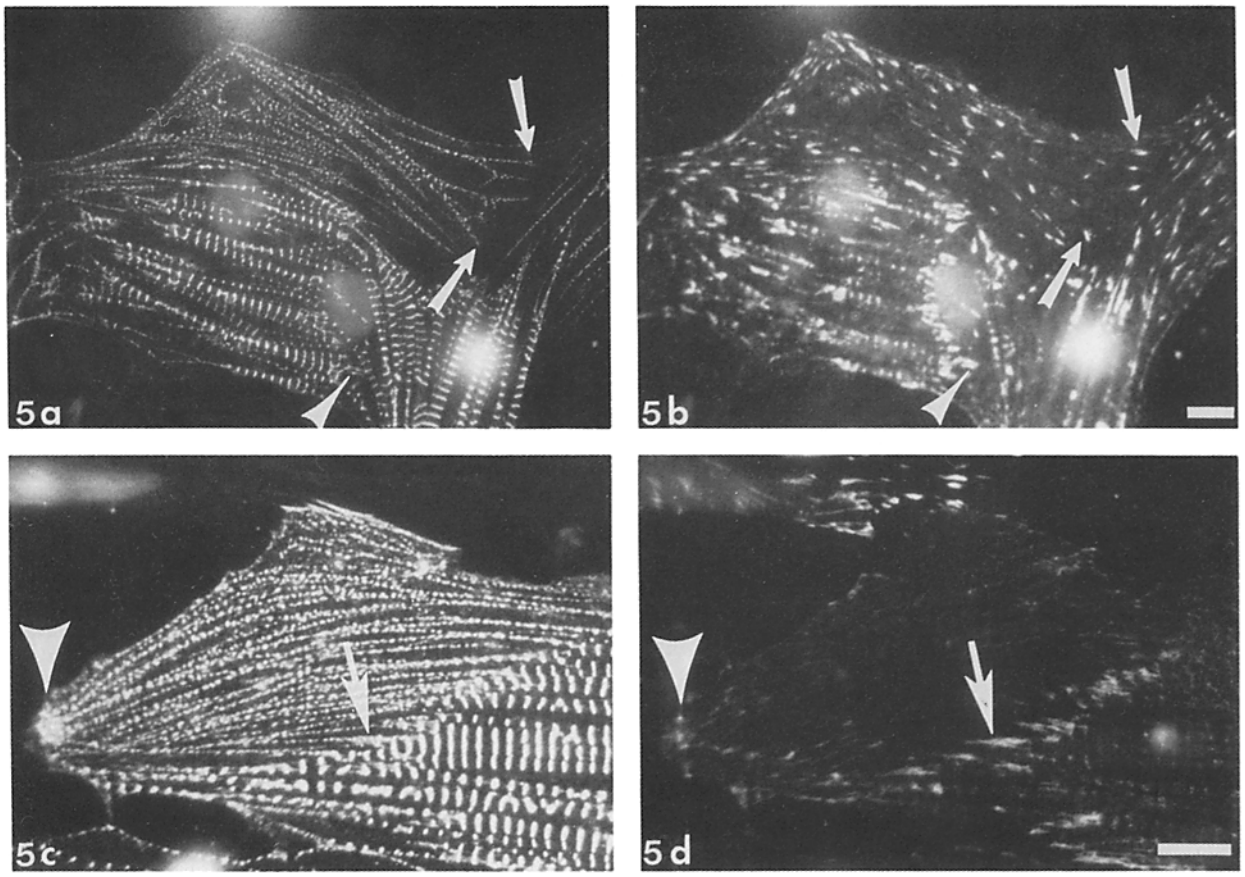

Figure 5. (*a–d*) Myocytes double-stained to reveal the multiple relationships of vinculin with NSMFs and SMFs. *a* and *c*, are stained with anti-α-actinin, (*fluorescein channel*), *b* and *d* with antivinculin (*rhodamine channel*). *a* and *b* show vinculin-containing adhesion plaques associated with both NSMFs (*arrows*) and SMFs (*arrowheads*). Costomere staining with antivinculin (*b*) varies greatly; frequently costomeres are not detected. In *c* and *d*, vinculin plaques are associated both with the termini of NSMFs (*arrowheads*) and SMFs, and with the NSMF/SMF transition zones (*arrows*). Slender vinculin positive plaques are found intermittently along the body of both NSMFs and SMFs. The circular fluorescent spots in *a* and *b* are due to DAPI bleed-through. Bars, 10 μm.

of stress fibers in cultured nonmuscle cells (15). Antivinculin also stains slender plaques along the length of immature SMFs and, in an irregular manner, costomeres (Fig. 5 *B*) (35). Vinculin positive adhesion plaques assemble along the cell's ventral surface, but never subtend ectopic α-actinin patches. The slender plaques along the body of the SMFs disappear as the myofibrils mature and are displaced from the cytocortical region into the interior of the cell (3, 11). Adhesion plaques are also found along the length of NSMFs and at their distal tips, and are particularly prominent at the transition zone between NSMFs and SMFs (Fig. 5, *C–D*).

These findings demonstrate that a structure approximating an in situ intercalated disk (e.g., subsarcolemmal vinculin/sarcomeric α-actinin/α-actin complex) assembles not only at a site of cell–cell contact (15, 30), but in apposition to a collagen substratum. By analogy to a hemidesmosome, this is a hemi-intercalated disk. It will be interesting to determine whether the plaques associated with NSMFs differ from those associated with the most distal sarcomeres of SMFs, and how similar both types of plaques are to intercalated disks.

Antibodies to Two Different Titin Epitopes Decorate Myocytes Differently

Anti-T20, which binds to a titin epitope at the Z-band in adult myofibrils (13), stains every narrow nascent Z-band in every nascent SMF (Fig. 6). The tight coupling between α-actinin and this titin epitope is such that, after double-staining, a given Z-band stained with anti-α-actinin cannot be resolved from that Z-band stained with anti-T20. This relationship includes those Z-bands that mark the distal margin of the terminal sarcomeres at the NSMF/SMFs transition sites (Fig. 6, *C* and *D*). The coupling between α-actinin and this titin epitope is further documented by the precise costaining of virtually every 0.3-μm aggregate in ectopic patches and in NSMFs by these two antibodies.

Anti-T1 stains an epitope on either side of each Z-band in mature myofibrils (13) and in SMFs in postmitotic, mononucleated skeletal myoblasts (18). Similarly, in cardiac myocytes every emergent ~1.7-μm sarcomere is characterized by a delicate titin-doublet flanking every Z-band (Fig. 7, *G* and *H*). Failure to resolve each titin band into a doublet is proba-

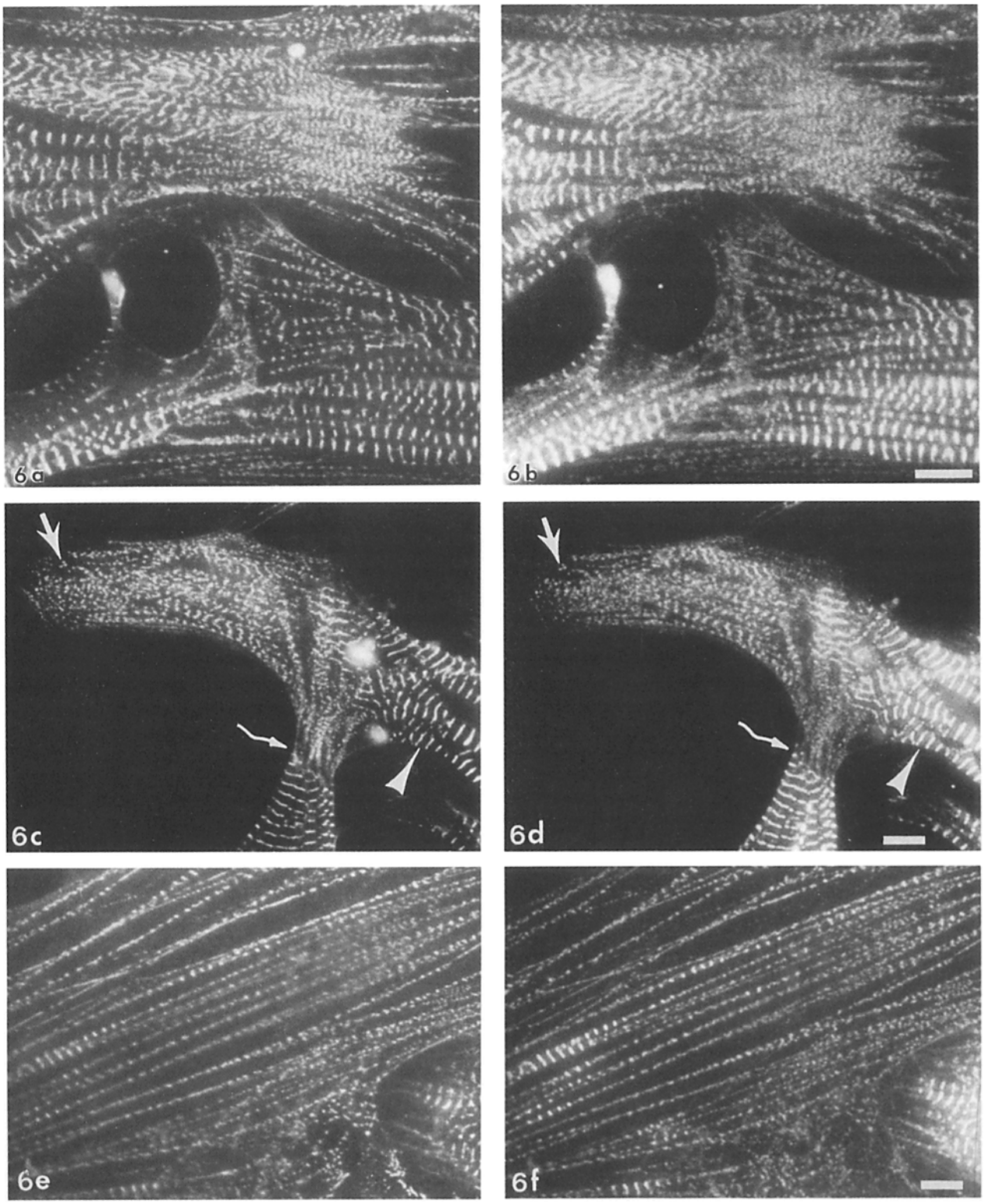

Figure 6. Cardiac myocytes double-stained with muscle specific α-actinin (*a*, *c*, and *e*, *fluorescein*) and anti-T20 to titin (*b*, *d*, *f*, *rhodamine*). Note the precise colocalization of α-actinin and titin in both the Z-lines of SMFs and the 0.3-μm aggregates of NSMFs and ectopic patches (*arrows*). In addition, for reasons not understood, anti-T20 also lightly stains the M-bands of SMFs (*d*, *arrowhead*). *a–d* illustrate the common multiple branching and crisscrossing of both NSMFs and SMFs in cardiac cells, whereas their arrangement in *e* and *f* is more similar to the parallel orientation of myofibrils typical of developing skeletal muscle. The wavy arrows in *c* and *d* point to the junction between two cardiac cells. Observe the terminal Z-band at this site. Bar, 10 μm.

bly because of partial contraction. Titin-doublets without a contained α-actinin Z-band have not been observed; conversely, narrow Z-bands have not been observed without flanking delicate titin-bands. In many instances the most terminal sarcomere, presumably the most recently assembled in a given SMF, can be identified by anti-T1 staining, not as a doublet, but as a singlet that is just proximal to the terminal α-actinin Z-band (Fig. 7, *G* and *H*). The strict correlation in size between any α-actinin Z-band and its associated titin bands is evident even in the barely resolvable titin-doublets indicated in Fig. 7, *E* and *F*.

In contrast to anti-T20, anti-T1 in most cells stains only the SMFs and does not stain ectopic patches or NSMFs (Fig. 7). In a few cells, anti-T1 lightly decorates the ectopic patches and NSMFs. Here, anti-T1 stains fine granules that are coextensive with the patches and NSMFs, but, unlike anti-T20, these do not exhibit a one-to-one correspondence with the 0.3-μm α-actinin aggregates. For unknown reasons, both anti-T20 and anti-T1 also variably stain the M-lines of SMFs (Fig. 6, *D* and *F*).

The quantitative relationship between α-actinin Z-bands and adjacent titin-bands extends to their spatial deployment as well. Cardiac myofibrils branch frequently (Fig. 1 *A* and *B*). Such branch points are often occupied by sizeable, amorphous α-actinin masses (Fig. 7 *G*). The shape and size of these streaming Z-bands varies, depending on the number of SMFs involved (27). Irrespective of shape or size, the atypical masses of α-actinin that function as Z-bands are faithfully costained over their entire area by anti-T20, and are outlined by delicate bands of anti-T1 (Fig. 7 *H*). Titin-T1 does not appear within the amorphous α-actinin structures, and the width of the spatially distorted T1 layer is that of a normal titin-singlet.

Myomesin and C-Protein Are Detected Only in SMFs

Anti-myomesin stains M-bands in cultured skeletal and cardiac myogenic cells (16). Because strikingly different staining patterns were obtained with different monoclonal antibodies to titin, we used three different monoclonal antibodies to localize myomesin. All three monoclonal antibodies to myomesin gave similar results. As shown in Fig. 8 (*A–D*) every α-actinin Z-band is associated with two flanking myomesin M-bands, with one interesting exception. The exception occurs in the terminal sarcomere of every SMF. The distal boundary of each terminal sarcomere is a sharp Z-band located ~1.7 μm from the penultimate Z-band (Figs. 3, *A* and *G*, 4 *A*, 7 *G*, 8, *A* and *C*). With respect to this terminal Z-band, there is a proximal myomesin M-band, but not a distal myomesin M-band (Fig. 8, *A–D*). This relationship obtains even to the just resolvable spots of myomesin illustrated in Fig. 8, *B* and *D*. It is also apparent from Fig. 8 (*A–D*) that myomesin is not detected in NSMFs or ectopic patches. Myomesin is detected only in M-bands which, in turn, are only found within the borders of ~1.7-μm sarcomeres.

Anti–C-protein has been shown to stain broad doublets within every A-band in adult as well as embryonic SMFs (33). Fig. 9 (*A* and *B*) demonstrates that this localization applies to cultured myocytes. Fig. 9 (*A* and *B*) also demonstrates that the distribution of C-protein parallels that of myomesin, in that it is absent from both NSMFs and ectopic patches. When detected it is always incorporated into a characteristic region within the confines of a given A-band.

Discussion

The findings in this report are based on static fluorescent images. Descriptive data of this kind do not readily lend themselves to mechanistic models of the steps in which newly synthesized myofibrillar proteins polymerize, translocate, assemble into intermediate structures such as I-Z-I–like complexes and MHC fibrils, and eventually stabilize as tandem sarcomeres with a minimal size of ~1.7 μm. Finding, however, that I-Z-I–like complexes and clusters of MHC fibrils can exist independently of one another, that at least one titin epitope is not detected in nonstriated structures, and that myomesin and C-protein staining are tightly linked with the assembly of sarcomeres are observations for which any model of myofibrillogenesis must account.

Earlier cytoimmunofluorescence and EM studies demonstrated that nascent SMFs consist, in addition to MHC thick filaments, of α-actinin Z-bands with inserted, polarized 1.0-μm-thin filaments positive for α-actin and sarcomeric tropomyosin (27, 46). What was not anticipated, however, was the extensive distribution of what we term I-Z-I–like complexes outside of the SMFs. I-Z-I–like complexes appear to consist of irregularly shaped ~0.3-μm α-actinin/titin aggregates associated with polymers of α-actin and with troponin-I. These I-Z-I–like complexes that stain with sarcomeric anti–α-actinin are morphologically indistinguishable from the ~0.3-μm α-actinin aggregates in stress fibers and ectopic patches in nonmuscle cells that stain with cytoskeletal anti–α-actinin (26, 38). Similarly, stress fibers and ectopic patches in nonmuscle cells stain continuously with rho-phalloidin and antibodies to the cytoskeletal actins, as do NSMFs and ectopic patches in myocytes stained with rho-phalloidin and antibodies to α-actin and troponin-I. The findings on stress fibers in nonmuscle cells are consistent with the notion that cytoskeletal α-actinin aggregates function as nucleation or organizing centers for the polymerization of thin filaments composed of cytoskeletal actins and tropomyosins. When assembled and extended, these complexes in nonmuscle cells would form stress fibers of linearly arranged, punctate α-actinin dense bodies and associated thin filaments (25). Analogous nucleation in myocytes involving the sarcomeric isoforms of α-actinin, α-actin, troponin-I, and titin may also lead to the assembly of numerous, I-Z-I–like complexes. Currently, we are attempting to determine the length and polarity of the actin polymers in the I-Z-I–like complexes in the NSMFs versus the ectopic patches, and whether they involve both cytoskeletal and sarcomeric isoforms.

The considerable differences in stoichiometry of the myofibrillar proteins in SMFs, NSMFs, and ectopic patches raise the issue of unstable intermediates. In mature SMFs the ratio by weight of α-actinin to MHC is roughly 1:20. It is not possible to relate this ratio directly to the respective fluorescent intensities in Figs. 3 and 4. Nevertheless, along the length of a given NSMF the quantity of MHC fibrils varies enormously, whereas that of the punctate α-actinin aggregates remains relatively constant. In the ectopic patches (Fig. 1 *F*; Fig. 3, *G* and *H*) MHC fibrils may be totally absent. The presence of I-Z-I–like complexes without accompanying MHC fibrils poses the question of whether all I-Z-I–like complexes are actually incorporated into sarcomeres. I-Z-I–like complexes may be assembled in great excess with many not available for incorporation into definitive sarcomeres. Excess I-Z-I–like complexes may be unstable and subject to

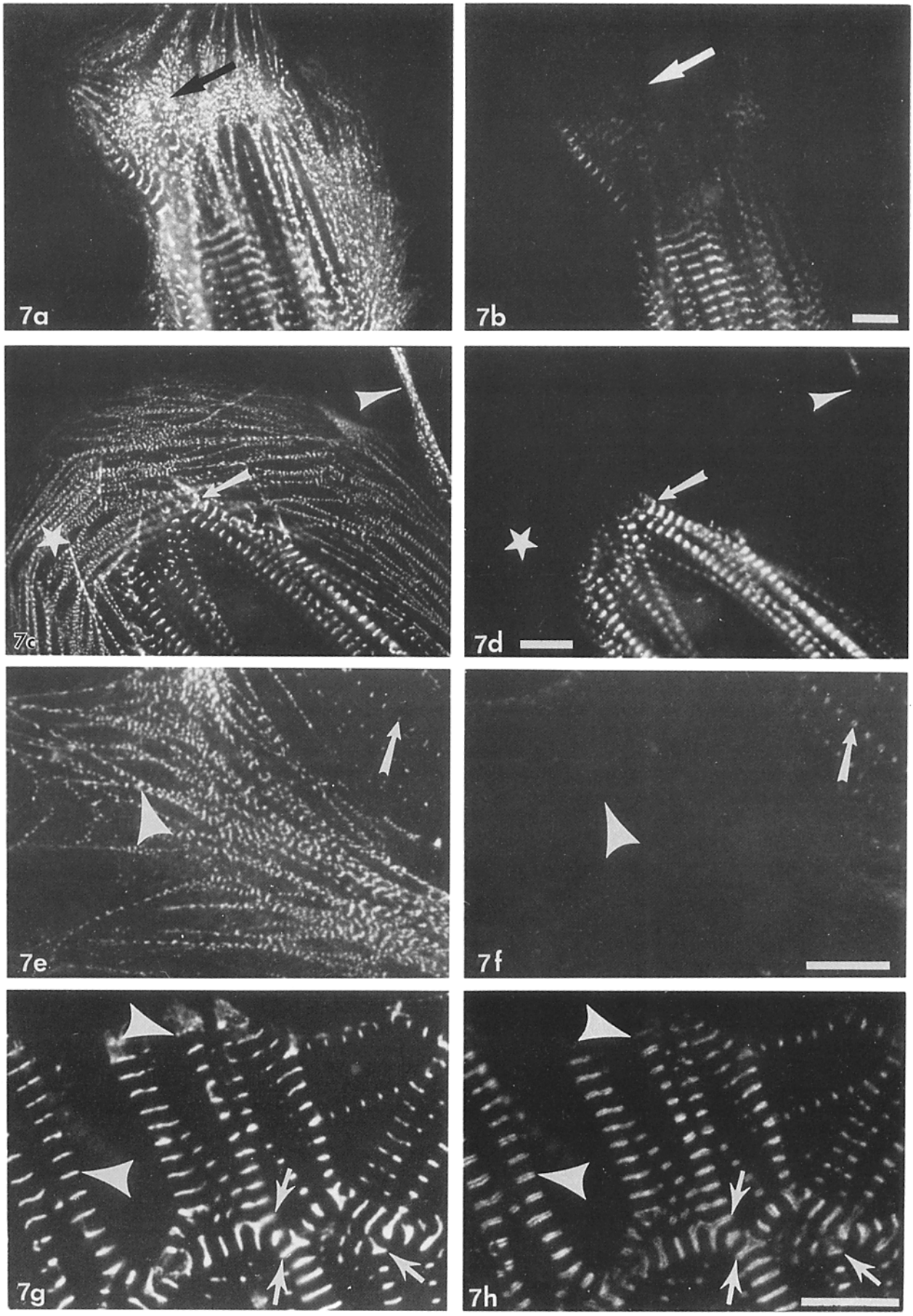
7a
7b
7c
7d
7e
7f
7g
7h

more rapid degradation than are the I-Z-I complexes stabilized in SMFs.

Finding I-Z-I–like complexes well separated from MHC fibrils suggests that these two structures can assemble independently of one another. Studies on skeletal cells treated with microtubule depolymerizing and stabilizing drugs have led to the same conclusions (2, 18, 22, 44) as have reports that *Drosophila* mutants lacking muscle actin nevertheless accumulate thick filaments and that mutants lacking MHC assemble I-Z-I–like complexes (5, 9).

Though the subject of recent papers (13, 17, 18, 44, 45, 46), the role of titin in myofibrillogenesis is still unclear. Hill et al. (18) stated that, although desmin could be detected in a subset of replicating presumptive skeletal myoblasts (10, 24), titin and MHC could be identified only in postmitotic, mononucleated myoblasts. Handel et al. (17) and Wang et al. (46) report that titin is primarily located in centrally located striated structures, with much less being associated with peripheral NSMFs. The use of monoclonal antititin antibodies allows us to probe more closely the relationship between titin and myofibrillar structures. The colocalization of anti-α-actinin and anti-T20 in ectopic patches and NSMFs (Fig. 6) strongly suggests that these two proteins are linked from the earliest stages of myofibrillogenesis and that this linkage occurs before the assembly of sarcomeres. The T1 epitope shows a significantly different pattern of distribution. Usually, no T1 is detectable in the 0.3-μm α-actinin aggregates (Fig. 7). On occasion, anti-T1 stains a fine granular pattern more or less coextensive with the NSMFs and ectopic patches, but not colocalizing, as does anti-T20, on a one-to-one basis with the ~0.3-μm aggregates. One interpretation for these disparate staining patterns is that, in I-Z-I–like complexes, titin is linked by its Z-band epitope to α-actinin, whereas the opposite or A-band end of the molecule is less constrained. The tethered T20-positive epitopes would then be concentrated in a smaller volume than the spread free ends containing the T1 epitope. The notion of the T1 end being free resulting in fewer epitopes per unit volume, could account for the numerous instances where anti-T1 failed to stain the ectopic patches or NSMFs. In other instances, where the titin molecules are packed or even partially aligned, the resulting higher density of T1 epitopes would permit their detection. Even under these conditions, however, they would not colocalize precisely with the α-actinin aggregates. Concurrent with sarcomere assembly, perhaps as a prerequisite, there must be a longitudinal alignment of titin, since even in the finest SMFs anti-T1 stains a delicate doublet around each Z-band (Fig. 7, *E* and *F*). It will be interesting to determine whether, during this brief period, while the Z-band end of titin is part of an I-Z-I–like complex, its free A-band end captures nearby thick filaments. An alternative explanation for the disparate titin staining patterns is that titin undergoes a conformational change just before becoming incorporated into a sarcomere, exposing the T1 epitope. With neither titin antibody do we detect any evidence that titin exhibits a sarcomeric pattern before alpha-actinin.

Most intriguing is the finding that myomesin and C-protein, which are present in their typical locations even in the most nascent sarcomeres, are undetectable in NSMFs, ectopic patches, or elsewhere in myocytes. Obviously at this time we cannot exclude the possibility that small numbers of myomesin or C-protein molecules do in fact associate with all or some MHC fibrils or other myofibrillar elements, but that they are too few to be detected by our techniques. It is also possible that the respective epitopes on myomesin or C-protein recognized by our mAbs are available only when each is appropriately folded and positioned within the confines of a ~1.7-μm sarcomere. Several observations, however, encourage the view that myomesin and C-protein are absent from nonstriated structures. (*a*) Three different monoclonal antibodies to myomesin give similar staining patterns. (*b*) On a molar basis, α-actinin, myomesin, and C-protein each constitute 1–4% of the SMFs. Yet α-actinin appears to be a major component in both NSMFs and ectopic patches with both monoclonal and polyclonal antibodies, whereas the others are not detectable. (*c*) The fine SMFs in Figs. 7 *F* and 8 *D* indicate that, when present, very small numbers of antigen molecules can be detected. Work in progress with other monoclonal and with polyclonal antibodies, with more concentrated antibodies combined with image intensification, and with different fixation protocols, should yield further information regarding the significance of the failure of our antibodies to detect myomesin or C-protein in ectopic patches and NSMFs.

More recently (8), we have been following myofibrillogenesis in the myotomes of stage 15–17 chick embryos (19), in conventional skeletal myogenic cultures (34), and in MyoD1-converted dermal fibroblasts, gizzard smooth muscle cells, chondroblasts, and retinal pigment cells (41). The distribution of myofibrillar proteins and desmin in the postmitotic, mononucleated myoblasts in these different preparations is basically similar to that described for cardiac myocytes. There

Figure 7. (*a–h*) Myocytes double-stained with anti-α-actinin (*a*, *c*, *e*, and *g*, *fluorescein*) and anti-T1 to titin (*b*, *d*, *f*, and *h*, *rhodamine*). Note how the presence and/or absence of titin marks the distinct boundary of a group of SMFs from their distal NSMFs. The arrows in *a* and *b* indicate an ectopic patch rich in α-actinin aggregates. Barely detectable titin-bands spaced at ~1.7-μm intervals approach these patches. If titin associates with the ± 0.3-μm α-actinin aggregates in such patches, this relationship is beyond the sensitivity of our procedures. The abrupt cut-off of the titin-positive stripes in *d* precisely coincides with the terminal narrow α-actinin Z-band in *c*. Note the total absence of titin staining among the numerous ± 0.3-μm α-actinin aggregates (*stars*) that arch over and extend beyond the SMFs. Arrowheads at right point to a long process of an adjacent cell containing NSMFs. *e* and *f* are relevant to the issue of detecting small quantities of antigen packaged into just resolvable microscopic structures. Note that the ± 0.3-μm α-actinin aggregates that occupy the center of these micrographs, a mixture of NSMFs and ectopic patches, are larger in size and stain more intensely than the fine α-actinin positive Z-bands indicated by the long arrows at the right. Note too that most of these just resolvable α-actinin Z-bands (*e*) are flanked by titin-doublets (*f*). *g* and *h* illustrate the strict correlation in size and shape of α-actinin in normal and atypical Z-bands and the adjacent titin stripes. Arrows point to atypical Z-bands and their corresponding spatially distorted titin bands. The top arrowheads point to a terminal α-actinin Z-band that is associated not with a titin doublet but with a titin singlet proximal to the Z-band. The left arrowheads point to titin doublets surrounding an α-actinin Z-band. Bars, 10 μm.

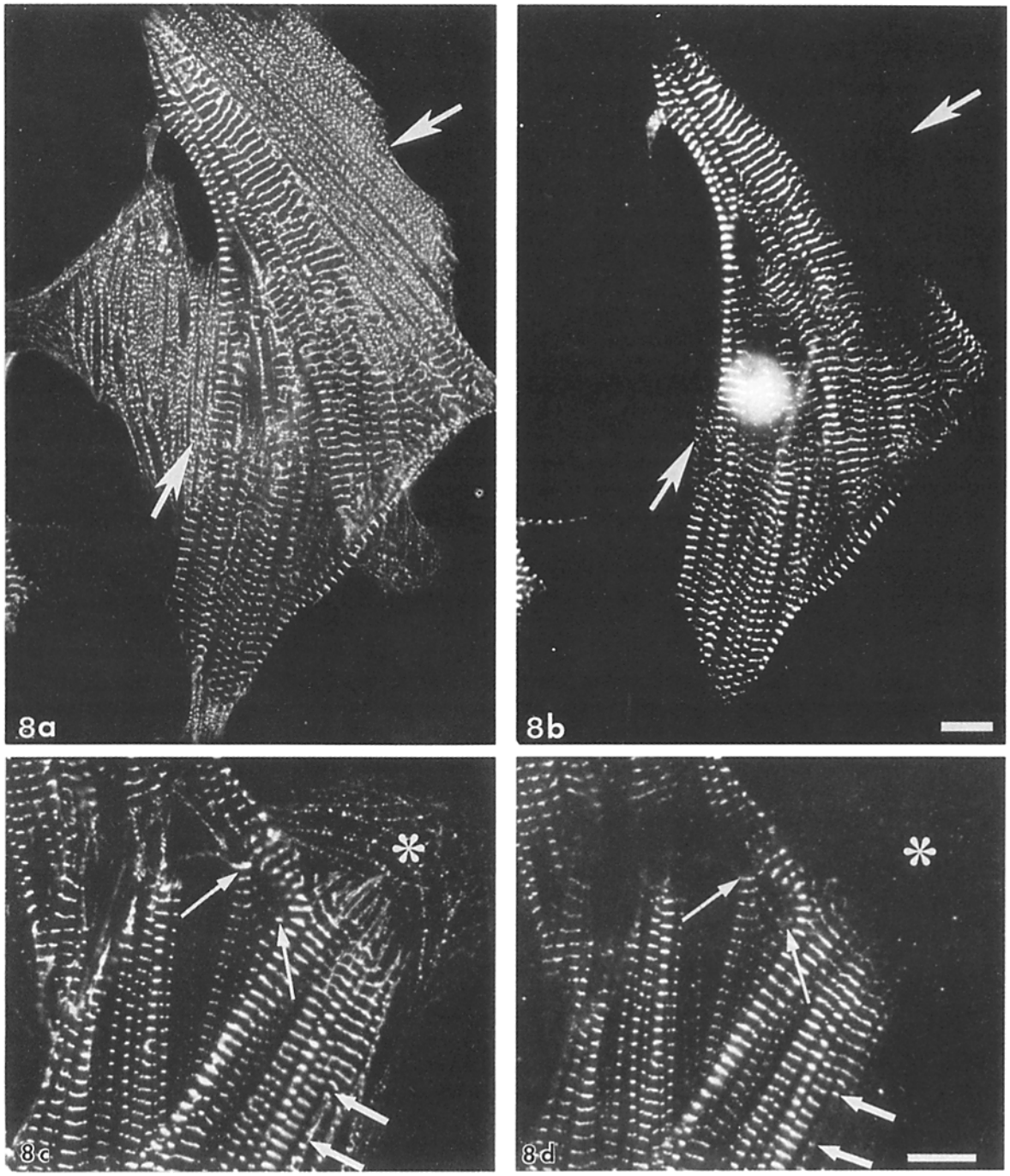

Figure 8. (*a–d*) The double-stained myocytes in *a* and *c* reveal the location of α-actinin (*fluorescein channel*), whereas those in *b* and *d* reveal the location of myomesin using mAb Cp-13 (*rhodamine channel*). Myomesin is only found in narrow M-bands that display a ~1.7-μm periodicity. (*a–b*) NSMFs and large ectopic patches, both densely packed with ± 0.3-μm α-actinin aggregates, do not stain with antimyomesin. Note the numerous examples of just perceptible SMFs. These consist of barely resolvable, longitudinally aligned myomesin bands with ~1.7-μm sarcomeric spacing that alternate with α-actinin spots having the same periodicity (*c–d*). The arrows are for purposes of orientation. The fluorescent circle in *b* is due to bleed-through of the Hoeschst-labeled nucleus. (*c–d*) The lower pair of arrows marks the terminal M-lines flanking an intercalated, nonstriated stretch. Note how the last myomesin-containing M-line is always followed by a terminal α-actinin-containing Z-band. The top arrow indicates a similar case, where the terminal M-band is followed by a terminal Z-band. The other narrow arrow is for orientation. Asterisks mark ectopic patches of α-actinin aggregates that lack corresponding myomesin staining. Numerous short NSMFs contain α-actinin but no myomesin. Bars, 10 μm.

are, however, some variations. For example, myomesin can be detected as a minor component in some NSMFs in postmitotic, mononucleated skeletal myoblasts and immature myotubes. However, there is no evidence that there is a sequence such that titin is assembled into a filamentous structure before the assembly of all other myofibrillar proteins or that the spatial distribution of titin presages individual sarcomeres before the assembly of other myofibrillar proteins (43).

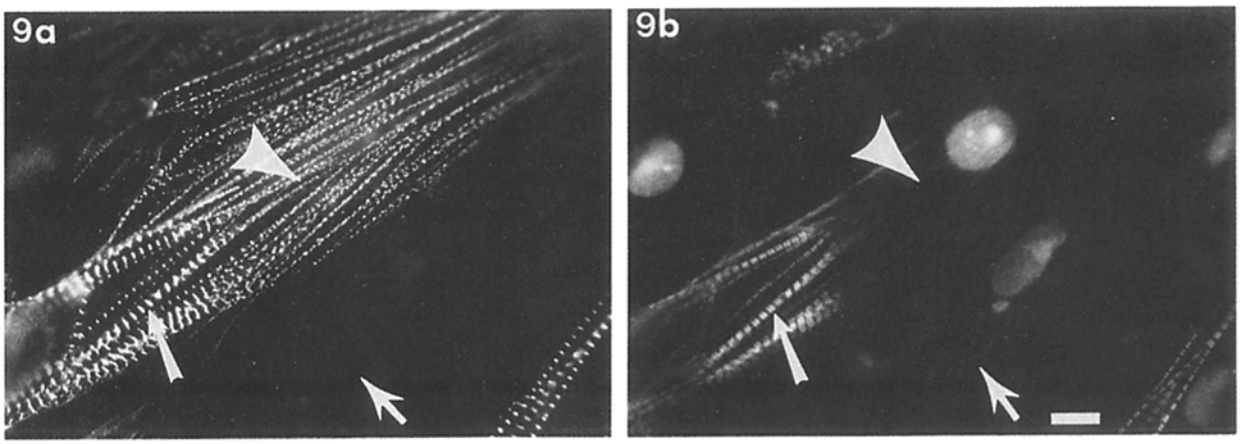

Figure 9. (*a–b*) Myocytes double stained with antibodies to α-actinin (*a, rhodamine*) and C-protein (*b, fluorescein*). Left arrows indicate SMFs, whereas arrowheads mark NSMFs. C-protein is detected only in the striated myofibrils. There is slight staining of the NSMFs with the C-protein antibody (*arrowheads*). However, since similar staining is found in nonmuscle cells (*right arrows*), the slight staining of the NSMFs is probably nonspecific. Bar, 10 μm.

Clearly, further studies using both cardiac and skeletal myogenic cells are required to define rules common to myofibrillogenesis in all types of myogenic cells, as well as rules unique to one or the other. For example, the insertion of the terminal sarcomeres of a given SMF into intercalated disks, or the frequent formation of streaming α-actinin Z-bands (Fig. 7, *G* and *H*) in various pathologies must involve events in cardiac cells not likely to occur in skeletal myogenic cells.

Central to the problem of myofibrillogenesis in both types of myogenic cells are the following: (*a*) what are the respective roles of such transient assemblies as stress fiber-like structures (3, 11, 29), ectopic patches, and NSMFs? (*b*) When and where does α-actinin first accumulate and with which thin filament proteins does it complex? and (*c*) what events occur at the boundary between NSMFs and SMFs and/or between an intercalated disk and a terminal sarcomere that result in the insertion of a de novo assembled sarcomere in the absence of an obvious morphogenetic gradient? Currently, we favor the notion that titin functions to splice elongating and relatively unstable I-Z-I-like complexes with equally unstable preformed 1.6-μm-long MHC-fibrils. The final packing of I-Z-I-like complexes and 1.6-μm-long MHC fibrils into ~1.7-μm sarcomeres probably requires the participation of myomesin and C-protein, and, at least in cardiac myocytes, submembraneous patches containing vinculin.

This work was supported by National Institutes of Health (NIH) grants Ca-18194, HL-15853, (to the Pennsylvania Muscle Institute), HD-07152, and HL-37675, 307-TT-0541528 and (from the Biomedical Research Support Grant Program); by the Muscular Dystrophy Association, and by the Research Foundation of the University of Pennsylvania. Part of this study was supported by an Alexander von Humboldt Senior Scientist Award (to H. Holtzer). T. Schultheiss is a trainee in the NIH-funded Medical Scientist Training Program, and is also supported by Cardiovascular Training grant 5-T32-HL-07502-10.

Received for publication 24 October 1989 and in revised form 18 December 1989.

References

1. Alema, S., and F. Tato. 1987. Interaction of retroviral oncogenes with the differentiation program of myogenic cells. *Adv. Cancer Res.* 49:1–28.
2. Antin, P., S. Forry-Schaudies, T. Friedman, S. Tapscott, and H. Holtzer. 1981. Taxol induces postmitotic myoblasts to assemble interdigitating microtubule-myosin arrays that exclude actin filaments. *J. Cell Biol.* 90:300–308.
3. Antin, P., S. Tokunaka, V. Nachmias, and H. Holtzer. 1986. Roles stress fiber-like structures in assembling nascent myofibrils in recovering ethyl methanesulfonate myosheets. *J. Cell Biol.* 102:1464–1479.
4. Atherton, B. T., D. M. Meyer, and D. G. Simpson. 1986. Assembly and remodeling of myofibrils and intercalated discs in cultured neonatal rat heart cells. *J. Cell Sci.* 86:233–248.
5. Beall, C. J., M. A. Sepanski, and E. A. Fryberg. 1989. Genetic dissection of *Drosophila* myofibril formation: effects of actin and myosin heavy chain null alleles. *Genes & Dev.* 3:131–140.
6. Bennett, G. S., S. Fellini, Y. Toyama, and H. Holtzer. 1979. Redistribution of intermediate filament subunits during skeletal myogenesis and maturation in vitro. *J. Cell Biol.* 82:577–584.
7. Blau, H. M., G. K. Pavalth, E. C. Hardeman, C. Chiu, L. Silberstein, S. G. Webster, S. C. Miller, and C. Webster. 1985. Plasticity of the differentiated state. *Science (Wash. DC).* 230:758–766.
8. Choi, J., T. Schultheiss, M. Lu, W. Franke, D. Bader, D. Fischman, and H. Holtzer. 1988. Founder cells for the cardiac and skeletal myogenic lineage. *In* Cellular and Molecular Biology of Muscle Development. F. Stockdale and L. Kedes, editors. Alan R. Liss, Inc., New York.
9. Chun, M., and S. Falkenthal. 1988. Ifm(2)2 is a myosin heavy chain allele that disrupts myofibrillar assembly only in the indirect flight muscle of *Drosophila melanogaster*. *J. Cell Biol.* 107:2613–2621.
10. Dlugosz, A. A., S. J. Tapscott, and H. Holtzer. 1983. Effect of phorbol 12-myristate 13-acetate on the differentiation program of embryonic chick skeletal myoblasts. *Cancer Res.* 43:2780–2789.
11. Dlugosz, A. A., P. Antin, V. Nachmias, and H. Holtzer. 1984. The relationship between stress fiber-like structures and nascent myofibrils in cultured cardiac myocytes. *J. Cell Biol.* 99:2268–2278.
12. Endo, T., and T. Masaki. 1984. Differential expression and distribution of chicken skeletal- and smooth-muscle type αactinins during myogenesis in culture. *J. Cell Biol.* 99:2322–2332.
13. Furst, D. O., M. Osborn, R. Nave, and K. Weber. 1988. The organization of titin filaments in the half-sarcomere revealed by monoclonal antibodies in immunoelectron microscopy: a map of ten nonrepetitive epitopes starting at the Z line extends close to a M line. *J. Cell Biol.* 106:1563–1572.
14. Fischman, D. 1986. Myofibrillogenesis and the morphogenesis of skeletal muscle. *In* Myology. A. Engle, and B. Banker, editors. McGraw-Hill Inc. New York. 1–32.
15. Geiger, B., T. Volk, and T. Volberg. 1985. Molecular heterogeneity of adherens junctions. *J. Cell Biol.* 101:1523–1531.
16. Grove, B., L. Cerny, J. Perriard, and H. Eppenberger. 1985. Myomesin and M-protein: expression of two M-band proteins in pectoral muscle and heart during development. *J. Cell Biol.* 101:1413–1421.
17. Handel, S. E., S.-M. Wang, M. L. Greaser, E. Schultz, J. Bulinski, and J. L. Lessard. 1989. Skeletal muscle myofibrillogenesis as revealed with a monoclonal antibody to titin in combination with detection of the α- and γ-isoforms of actin. *Dev. Biol.* 132:35–44.
18. Hill, C. S., S. Duran, Z. Lin, K. Weber, and H. Holtzer. 1986. Titin and myosin, but not desmin are linked during myofibrillogenesis in postmitotic mononucleated myoblasts. *J. Cell Biol.* 103:2185–2196.
19. Holtzer, H., J. Marshall, and H. Finck. 1957. An analysis of myogenesis by use of fluorescent antimyosin. *J. Biophys. Biochem. Cytol.* 3:705–

725.
20. Holtzer, H., J. Sanger, H. Ishkawa, and K. Strahs. 1972. Selected topics in skeletal myogenesis. *Cold Spring Harbor Symp. Quant. Biol.* 37:549–566.
21. Holtzer, H., J. Biehl, G. Yeoh, N. Meganathan, and A. Kaji. 1975. Effect of oncogenic virus on muscle differentiation. *Proc. Natl. Acad. Sci. USA.* 72:4051–4055.
22. Holtzer, H., J. Croop, Y. Toyama, B. Bennett, S. Fellinin, and C. West. 1979. Differences in differentiation programs between presumptive myoblasts and their daughters, the definitive myoblasts and myotubes. *In* Plasticity of Muscle. D. Pette, editor. Walter de Gruyter & Co., Berlin.
23. Ishikawa, H., R. Bischoff, and H. Holtzer. 1968. Formation of arrowhead complexes with heavy meromyosin in a variety of cell types. *J. Cell Biol.* 43:312–323.
24. Kaufman, S. J., and R. F. Foster. 1988. Replicating myoblasts express a muscle-specific phenotype. *Proc. Natl. Acad. Sci. USA.* 85:9606–9610.
25. Langanger, G., M. Moeremans, G. Daniels, M. DeBrander, and J. DeMay. 1986. The molecular organization of myosin in stress fibers of cultured cells. *J. Cell Biol.* 102:200–209.
26. Lazarides, E., and K. Burridge. 1975. α-actinin: immunofluorescent localization of a muscle structural protein in non-muscle cells. *Cell.* 6:289–298.
27. Legato, J. 1972. Ultrastructural characteristics of the rat ventricular cell grown in tissue-culture with special reference to sarcomerogenesis. *J. Mol. Cell Cardiol.* 4:209–317.
28. Lessard, J. L. 1988. Two monoclonal antibodies to actin; one generally reactive and the other muscle selective. *Cell Motil. Cytoskeleton.* 10:349–362.
29. Lin, Z., J. Eshelman, C. Grund, D. A. Fischman, T. Masaki, W. W. Franke, and H. Holtzer. 1989. Differential response of myofibrillar and cytoskeletal proteins in cells treated with phorbol myristate acetate. *J. Cell Biol.* 108:1079–1091.
30. Lin, Z., S. Holtzer, T. Schultheiss, J. Murray, T. Masaki, D. A. Fischman, and H. Holtzer. 1989. Polygons and adhesion plaques and the disassembly and assembly of myofibrils in cardiac myocytes. *J. Cell Biol.* 108:2355–2367.
31. Markwald, R. R. 1973. Distribution and relationship of precursor Z material to organizing myofibrillar bundles in embryonic rat and hamster ventricular myocytes. *J. Mol. Cell. Cardiol.* 5:341–350.
32. McKenna, N. M., C. S. Johnson, and Y. Wang. 1986. Formation and alignment of Z lines in living chick myotubes microinjected with rhodamine-labeled alpha-actinin. *J. Cell Biol.* 103:2163–2171.
33. Obinata, A., S. Kitani, T. Masaki, and D. Fischman. 1984. Co-existence of fast-type and slow-type C-proteins in neonatal chicken breast muscle. *Dev. Biol.* 105:253–256.
34. Okazaki, K., and H. Holtzer. 1965. An analysis of myogenesis in vitro using fluorescein-labelled antimyosin. *J. Cytol. Histochem.* 13:726–739.
35. Pardo, J., J. D'Angelo, and S. Craig. 1983. Vinculin is a component of an extensive network of myofibril-sarcolemma attachment regions in cardiac muscle fibers. *J. Cell Biol.* 97:1081–1088.
36. Peng, H. B., J. J. Wolosewick, and P.-C. Cheng. 1981. The development of myofibrils in cultured muscle cells: a whole-mount and thin-section electron microscopic study. *Dev. Biol.* 88:121–136.
37. Pette, D., and G. Vrbova. 1985. Invited review: neural control of phenotypic expression in mammalian muscle fibers. *Muscle & Nerve.* 8:676–689.
38. Rathke, P. C., M. Osborn, and K. Weber. 1979. Immunological and ultrastructural characterization of microfilaments bundles; polygonal nets and stress fibers in an established cell line. *Eur. J. Cell Biol.* 19:40–48.
39. Rubinstein, N., G. Lyons, and A. Kelly. 1988. Hormonal control of myosin heavy chain gene during development of skeletal muscle. Plasticity of the neuromuscular system. *Ciba Found. Symp.* 138:35–51.
40. Sanger, J. M., B. Mittal, M. B. Pochapin, and J. W. Sanger. 1986. Myofibrillogenesis in living cells microinjected with fluorescently labelled alpha-actinin. *J. Cell Biol.* 102:2053–2066.
41. Tapscott, S. J., A. B. Lassar, and H. Weintraub, 1989. 5-bromo-2'-deoxyuridine blocks myogenesis by extinguishing expression of MyoD1. *Science (Wash. DC).* 245:532–536.
42. Terai, M., M. Komiyama, and Y. Shimada, 1989. Myofibril assembly is linked with vinculin, α-actinin, and cell-substrate contacts in embryonic cardiac myocytes in vitro. *Cell Motil. Cytoskeleton.* 12:185–194.
43. Tokuyasu, K. T., and P. A. Maher. 1987. Immunocytochemical studies of cardiac myofibrillogenesis in early chick embryos. I. Presence of immunofluorescent titin spots in premyofibril stages. *J. Cell Biol.* 105:2781–2793.
44. Toyama, Y., S. Forry-Schaudies, B. Hoffman, and H. Holtzer. 1982. Effect of taxol and colcemid on myofibrillogenesis. *Proc. Natl. Acad. Sci. USA.* 79:6556–6566.
45. Wang, K. 1982. Myofilamentous and myofibrillar connections: role of titin, nebulin and intermediate filaments. *In* Muscle Development, Molecular and Cellular Control. M. L. Person and H. F. Epstein, editors. Cold Spring Harbor Laboratory, Cold Spring Harbor, New York. 439–452.
46. Wang, S.-M., M. L. Greaser, E. Schultz, J. C. Bulinski, J. J.-C. Lin, and J. L. Lessard. 1988. Studies on cardiac myofibrillogenesis with antibodies to titin, actin, tropomyosin, and myosin. *J. Cell Biol.* 107:1075–1083.
47. Zadeh, B. J., A. Gonzales-Sanchez, D. A. Fischman, and D. M. Bader. 1986. Myosin heavy chain expression in embryonic cardiac cell cultures. *Dev. Biol.* 155:204–214.